will be a substantial delay in the impact of lower crustal production rates on decreased low-temperature fluid fluxes, because the age spectrum of the ridge flanks changes only slowly. Presently, only ~55% of the ocean floor is less than 65 million years old and contributes to ridge flank hydrothermal circulation, compared with ~85% in the Late Cretaceous (*32*). Decreasing fluid-rock exchange on the ridge flanks throughout the Tertiary, superimposed on decreases in global mid-ocean ridge axial hydrothermal activity since the Cretaceous, could therefore explain the observed increase in seawater Mg/Ca and Sr/Ca ratios since the Oligocene.

References and Notes

1. J. W. Morse, Q. W. Wang, M. Y. Tsio, *Geology* **25**, 85 (1997).
2. A. L. Cohen, K. E. Owens, G. D. Layne, N. Shimizu, *Science* **296**, 331 (2002).
3. C. H. Lear, H. Elderfield, P. A. Wilson, *Science* **287**, 269 (2000).
4. C. H. Lear, H. Elderfield, P. A. Wilson, *Earth Planet. Sci. Lett.* **208**, 69 (2003).
5. R. A. Berner, A. C. Lasaga, R. M. Garrels, *Am. J. Sci.* **283**, 641 (1983).
6. F. T. Mackenzie, R. M. Garrels, *Am. J. Sci.* **264**, 507 (1966).
7. S. J. Carpenter *et al.*, *Geochim. Cosmochim. Acta* **55**, 1991 (1991).
8. J. A. D. Dickson, *Science* **298**, 1222 (2002).
9. C. H. Lear, Y. Rosenthal, N. Slowey, *Geochim. Cosmochim. Acta* **66**, 3375 (2002).
10. T. Steuber, J. Veizer, *Geology* **30**, 1123 (2002).
11. J. Horita, H. Zimmerman, H. D. Holland, *Geochim. Cosmochim. Acta* **66**, 3733 (2002).
12. T. K. Lowenstein, M. N. Timofeeff, S. T. Brennan, L. A. Hardie, R. V. Demicco, *Science* **294**, 1086 (2001).
13. M. N. Timofeeff, T. K. Lowenstein, M. A. Martins da Silva, N. B. Harris, *Geochim. Cosmochim. Acta* **70**, 1977 (2006).
14. F. M. Richter, D. J. DePaolo, *Earth Planet. Sci. Lett.* **83**, 27 (1987).
15. Materials and methods are available as supporting material on *Science* Online.
16. H. Elderfield, C. G. Wheat, M. J. Mottl, C. Monnin, B. Spiro, *Earth Planet. Sci. Lett.* **172**, 151 (1999).
17. J. C. Alt, D. A. H. Teagle, *Geochim. Cosmochim. Acta* **63**, 1527 (1999).
18. R. M. Coggon, D. A. H. Teagle, M. J. Cooper, D. A. Vanko, *Earth Planet. Sci. Lett.* **219**, 111 (2004).
19. J. M. McArthur, R. J. Howarth, T. R. Bailey, *J. Geol.* **109**, 155 (2001).
20. A. T. Fisher *et al.*, *Nature* **421**, 618 (2003).
21. P. A. Sandberg, *Nature* **305**, 19 (1983).
22. S. M. Stanley, L. A. Hardie, *Palaeogeogr. Palaeoclimatol. Palaeoecol.* **144**, 3 (1998).
23. F. M. Richter, Y. Liang, *Earth Planet. Sci. Lett.* **117**, 553 (1993).
24. T. Steuber, *Int. J. Earth Sci.* **88**, 551 (1999).
25. A. K. Tripati, W. D. Allmon, D. E. Sampson, *Earth Planet. Sci. Lett.* **282**, 122 (2009).
26. D. W. Lea, T. A. Mashiotta, H. J. Spero, *Geochim. Cosmochim. Acta* **63**, 2369 (1999).
27. U. Brand, A. Logan, N. Hiller, J. Richardson, *Chem. Geol.* **198**, 305 (2003).
28. P. S. Freitas, L. J. Clarke, H. Kennedy, C. A. Richardson, F. Abrantes, *Geochim. Cosmochim. Acta* **70**, 5119 (2006).
29. M. T. Gibbs, L. R. Kump, *Paleoceanography* **9**, 529 (1994).
30. K. L. Von Damm, *Geophys. Monogr.* **91**, 222 (1995).
31. R. D. Müller, M. Sdrolias, C. Gaina, B. Steinberger, C. Heine, *Science* **319**, 1357 (2008).
32. M. Seton, C. Gaina, R. D. Müller, C. Heine, *Geology* **37**, 687 (2009).
33. H. J. Paul, K. M. Gillis, R. M. Coggon, D. A. H. Teagle, *Geochem. Geophys. Geosyst.* **7**, Q02003 (2006).
34. J. Gaillardet, B. Dupré, P. Louvat, C. J. Allègre, *Chem. Geol.* **159**, 3 (1999).
35. M. Meybeck, A. Ragu, *River Discharges to the Oceans. An Assessment of Suspended Solids, Major Ions, and Nutrients, Environment Information and Assessment Report* (United Nations Environment Programme, Nairobi, Kenya, 1996).
36. D. Vance, D. A. H. Teagle, G. L. Foster, *Nature* **458**, 493 (2009).
37. This research was supported by National Environment Research Council research grants NER/T/S/2003/00048 and NE/E001971/1 to D.A.H.T. and NE/C513242/1 to R.M.C. and D.A.H.T. This research used samples provided by the Ocean Drilling Program (ODP) and the Integrated Ocean Drilling Program (IODP). ODP was sponsored by NSF and participating countries under the management of Joint Oceanographic Institutions. IODP is supported by NSF; Japan's Ministry of Education, Culture, Sports, Science and Technology; the European Consortium for Ocean Drilling Research; and the People's Republic of China, Ministry of Science and Technology. We thank M. Palmer, P. Wilson, D. Vance, R. James, and three anonymous reviewers for insightful comments that greatly improved this manuscript.

Climate-Modulated Channel Incision and Rupture History of the San Andreas Fault in the Carrizo Plain

Lisa Grant Ludwig,[1]* Sinan O. Akçiz,[1] Gabriela R. Noriega,[1] Olaf Zielke,[2] J Ramón Arrowsmith[2]

The spatial and temporal distribution of fault slip is a critical parameter in earthquake source models. Previous geomorphic and geologic studies of channel offset along the Carrizo section of the south central San Andreas Fault assumed that channels form more frequently than earthquakes occur and suggested that repeated large-slip earthquakes similar to the 1857 Fort Tejon earthquake illustrate typical fault behavior. We found that offset channels in the Carrizo Plain incised less frequently than they were offset by earthquakes. Channels have been offset by successive earthquakes with variable slip since ~1400. This nonuniform slip history reveals a more complex rupture history than previously assumed for the structurally simplest section of the San Andreas Fault.

Knowledge of the age and associated slip distribution for surface-rupturing earthquakes is essential for understanding fault rupture and the recurrence of large, potentially destructive earthquakes (*1*). Paleoseismological data about previous large earthquakes are needed to characterize rupture patterns and assess the associated seismic hazard (*2*). Dates of past earthquakes are obtained from excavations across active faults, where the disruption of the ground surface at the time of the event is encased in datable sediments. Channels offset along faults are used as markers to determine displacements in successive earthquakes and to infer earthquake recurrence on the basis of two assumptions: (i) Strain release rate along that section of the fault is constant during the period of interest, and (ii) the channels form more frequently than they are offset by earthquakes.

The south central San Andreas Fault (SAF) last ruptured in the great 1857 earthquake (all dates are calendar years C.E.) and displaced channels that crossed the fault (*3*, *4*). In the Carrizo Plain, measurements of slip rate over different time intervals agree with geodetically measured loading rates of ~35 mm/year (*2*, *3*, *5*). Several studies have analyzed offset channels to infer slip distribution from the great 1857 earthquake and prior ruptures (*3*, *4*, *6–8*) in the semi-arid Carrizo Plain. Near Wallace Creek (Fig. 1), channels offset by approximately 33 m, 21.8 m, and 9.5 m (*3*, *4*) were interpreted to be caused by three successive earthquakes with surface slip of 11.2 m, 12.3 m, and 9.5 m, respectively (*3*). However, determining the incision age of offset ephemeral stream channels is difficult if only the channel fill sediments are dated, because transported organic material may have inherited age (*7*, *9–12*).

We sought to determine the age, and consequently the slip history, of channels that are offset by commonly measured offset values of ~8 to 10 m and ~16 m in the Carrizo Plain and along the 1857 rupture of the southern SAF (*4*, *7*, *8*). To test the hypothesis that incision occurred more frequently than offset, we used traditional stratigraphic analysis, with high-resolution radiocarbon dating and new records of extreme climate events (*9*, *13*, *14*), to determine the relative sequence of earthquake rupture and channel incision. We focused on a section of the SAF between Wallace
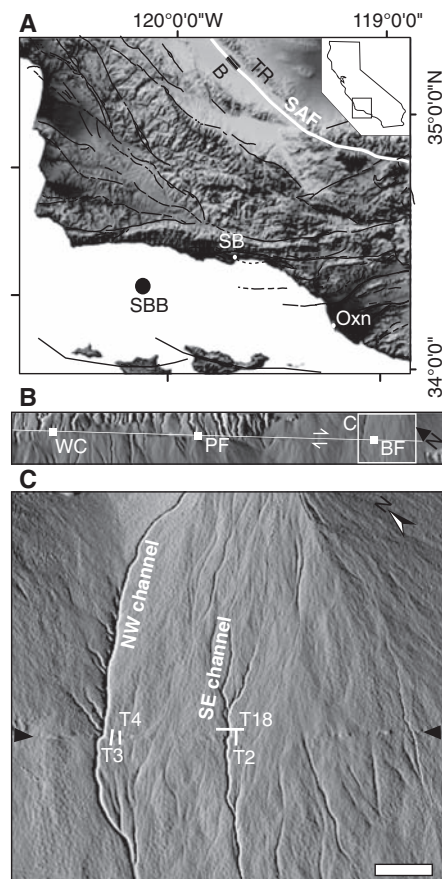
[1]Program in Public Health and California Institute for Hazards Research, University of California, Irvine, CA 92697, USA. [2]School of Earth and Space Exploration, Arizona State University, Tempe, AZ 85287, USA.

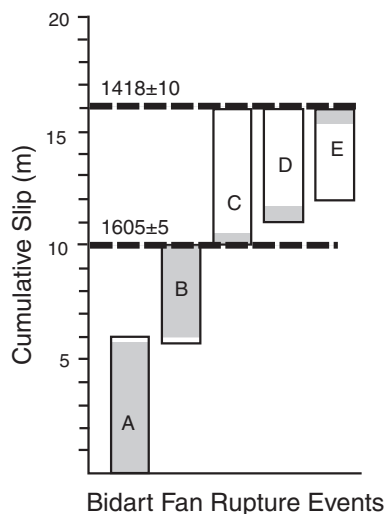*To whom correspondence should be addressed. E-mail: lgrant@uci.edu

Creek and the Bidart Fan (BF) paleoseismic site (Figs. 1 and 2) in the northern Carrizo Plain (7, 10–12), where excavations provide unique exposures of faulted sediment adjacent to offset channels (11, 15).

In the BF, drainage from the Temblor Range deposits alluvial sediments and forms channels nearly perpendicular to the SAF (Fig. 1). Drainage areas of these channels vary over several orders of magnitude along strike of the fault. BF shows evidence of recent deposition and incision of two offset channels (Fig. 1). Deposition of sediment on the BF surface and erosion of channels into it was driven by varying climatic conditions over the past 700 years (9). Many non-offset channels that now cross the SAF in the Carrizo Plain might have incised during the unusually wet decades from 1861 to 1891, possibly during 1861–1862, when floodwaters cut arroyos in southern California (16). Stratigraphic correlation and radiocarbon dating of sediments across the fan show that alluvium deposition was strongly controlled by incision of deep channels into the BF (17). The location of the depositional lobe has shifted through time (11), and those sections of the fan with deep channels experienced limited sedimentation. These incision events caused depositional hiatuses on the fan surface near the northwest and southeast channels (Fig. 1). Alluvial sediments that were deposited before incision of the adjacent (>2 m) deep channels were exposed in trenches 2, 3, and 4 (Fig. 1) and radiocarbon-dated to constrain the approximate dates of incision. Near the northwest channel, layers exposed in trenches 3 and 4 that are ~10 cm, ~50 cm, and ~60 cm below the surface were dated approximately 1340 to 1400 (15, 17), indicating that most deposition ceased around 1400 or later. Likewise, near the southeast channel, radiocarbon dates of detrital samples from the channel fill and alluvial deposits 20 to 30 cm below the fan surface indicate that incision occurred approximately 1616 to 1771 (17).

Fig. 1. (**A**) The San Andreas fault (SAF; white) and Quaternary faults (black) in southwestern California (SB, Santa Barbara; Oxn, the coastal region near Oxnard; SBB, the offshore Santa Barbara Basin). TR, Temblor Range; SAF region shown in (B) is indicated. (**B**) Hillshade map generated from LIDAR-based digital elevation map, showing the geomorphic expression of strike-slip faulting in the Carrizo Plain in the study area from Wallace Creek (WC) and Phelan Fan (PF) to Bidart Fan (BF). (**C**) A portion of the Bidart Fan zoomed in on the hillshade plot (grid size 0.5 m) showing southwest-flowing alluvial drainage system bisected by the northwest-trending SAF (between black triangles), which offsets two incised channels (NW and SE). Samples for radiocarbon dating were collected from three trenches (T2, T3, and T4) and the southeast channel (T18) for determining age of channel incision and surface abandonment (17). Scale bar, 200 m.

Fig. 2. Summary of cumulative slip, incision model, and slip per earthquake at BF. Five earthquakes and two incision events occurred since ~1400. Slip per earthquake is shown as shaded vertical bar, with maximum slip in open bars. The northwest channel is offset 15.9 m by five earthquakes (Table 1). The 1857 earthquake A generated 5.8 to 6.0 m of slip at BF. Total slip of the 1857 and penultimate earthquake B, 10.2 m, is constrained by offset of the southeast channel, incised around 1605 ± 5 (black dashed line). Three prior earthquakes (boxes labeled 3, 4, and 5) collectively offset the northwest channel as much as 5.6 m. Slip was at least 50 cm each (shaded bars).

Paleoclimate data provide an environmental context for interpreting alluvial deposits and identifying fluvial events that could have caused channel incision. High-resolution paleoclimate proxy data (9, 13, 14, 18) between 1300 and 1857 show that two prehistoric extreme flooding events eroded sediment from the coastal region near the Carrizo Plain and deposited sediment in anoxic basins offshore (13, 14). Cores from the offshore Santa Barbara Basin (SBB, Fig. 1) contain two unusually thick layers of terrigenous sediment deposited by floods from the Coast Ranges during the years 1605 ± 5 and 1418 ± 10. The extreme floods in ~1605 and ~1418 have been linked to extreme ENSO (El Niño–Southern Oscillation) events and global reorganizations of atmospheric circulation that left recognizable evidence from California to South America (14). In coastal central California, ENSO events are associated with unusually high precipitation and streamflow within ~100 km of the coast (18), which includes the Carrizo Plain. Extreme floods in the Santa Clara and Ventura watersheds (draining to the SBB) most likely also occurred in the Carrizo and could have left recognizable sedimentary or geomorphic evidence. Radiocarbon ages of near-surface sediments at BF are consistent with incision of the northwest channel in the ~1418 extreme coastal flooding event, and with incision of the southeast BF channel in the ~1605 extreme flooding event or shortly thereafter (17).

These incision ages are also consistent with the offset and apparent ages of the BF channels. Assuming a constant slip rate (2, 3, 5, 19), the southeast BF channel should have accumulated 8.8 m of slip between 1605 and 1857. Likewise, the northwest BF channel should have accumulated 15.4 m of slip between 1418 and 1857. Recent LIDAR (light detection and ranging)–based measurements show that the northwest channel is offset by ~15.9 m and the southeast channel is offset by ~10.2 m (8). Ground-based measurements of the southeast channel offset are 7 to 10 m (17). Excavations of buried offset channels near Wallace Creek yielded similar offset measurements for two channels—7.8 to 8.0 m and 15.1 to 15.8 m (12)—which suggests that they could have incised during these regional flooding events.

If the southeast BF channel incised around 1605, it must have been displaced by at least two earthquakes (15) instead of a single event, as initially assumed (4, 10, 11). LIDAR analysis results suggest that average slip during the 1857 earthquake in the Carrizo Plain was 5.3 ± 1.4 m (8), although it may have been as high as 6.9 m at the nearby Phelan Fan site (10). To account for possible slip variability, we interpolate BF slip as the average of the two nearest offset channels, which measured 6 ± 1 m (~750 m northwest of BF) and 5.8 ± 0.5 m (8) (2 km southeast of BF). Subtracting this amount, 5.9 ± 0.6 m, from the total offset of the southeast channel (10.2 ± 1.2 m), we obtain 4.3 ± 1.3 m of slip at BF from the penultimate earthquake. Similarly, correlating

Table 1. Bidart Fan earthquake sequence, channel incision, and offset events.

Earthquake date*	Inferred incision date	Channel	Total offset (m)	Number of offsets
(A) 1857			5.9	
(B) 1631–1823				
	1605 ± 5	SE	10.2†	2§
(C) 1547–1617§				
(D) ~1450–1547‡				
(E) ~1450–1547‡				
	1418 ± 10	NW	15.9†	5
(F) 1360–1425#				
(G) 1280–1340				

*Dates from (15) except as noted. Earthquake F is rupture event BDT4-d at trench T4. Earthquake G is rupture BDT4-e at T4. Earthquakes BDT3-f and BDT3-g at T3 (15) are older than earthquakes F and G in this table. †Measurements from (8). ‡Approximate age (21). §Inferred incision age of southeast channel overlaps with dates of second and third earthquakes reported by Akçiz et al. (15). They presented evidence that event BDT2-b is the third oldest earthquake, event C, and predates incision. New radiocarbon dates of BDT2-b (17) eliminate age overlap of earthquakes B and C. #The sixth earthquake, F, caused surface rupture between deposition of two near-surface sedimentary units (17) and therefore is inferred to predate incision of the adjacent northwest channel.

same-age sediments in trenches ~ 200 m away suggests that the northwest channel has been displaced by five surface ruptures (Table 1). Ages of sediments and their stratigraphic position in trench 4 support an interpretation of incision between the fifth and sixth earthquakes, during a time interval that includes the ~1418 extreme flood (17) (Table 1). Thus, the northwest channel has been offset in three additional earthquakes by as much as 5.6 m more than the offset of the southeast channel (Fig. 2). Slip in individual earthquakes at the BF is not directly measurable, but we can assume at least 50 cm of slip on the basis of expression in trench exposures (15). With minimum slip of 1 m in two earthquakes, maximum slip would be 4.6 m in the other earthquake.

Comparison of channel incision dates with the rate of occurrence of surface ruptures suggests that channel incision events are less frequent than earthquakes in the Carrizo Plain, which implies that some channels have been offset by more earthquakes than previously thought (9). Our observations do not support previous interpretations of ~9 m of slip in the 1857 earthquake (3, 4) or any of the earthquakes that ruptured since 1400. However, slip in the 1857 earthquake was apparently greater than in any of the four prior ruptures. This variable slip history is not consistent with repeated characteristic slip (20) at BF in the Carrizo, one of two areas where characteristic slip was defined (6). Since the 1857 earthquake, >5 m of strain has accumulated in the Carrizo, an amount greater than or similar to slip released in the last five ruptures.

References and Notes

1. Ch. H. Scholz, *The Mechanics of Earthquakes and Faulting* (Cambridge Univ. Press, Cambridge, ed. 2, 2002).
2. Working Group on California Earthquake Probabilities, *The Uniform California Earthquake Rupture Forecast, v2*, USGS Open File Report 2007 (2008).
3. K. E. Sieh, R. H. Jahns, *Geol. Soc. Am. Bull.* **95**, 883 (1984).
4. K. E. Sieh, *Bull. Seismol. Soc. Am.* **68**, 1421 (1978).
5. G. Schmalzle, T. Dixon, R. Malservisi, R. Govers, *J. Geophys. Res.* **111**, B05403 (2006).
6. D. P. Schwartz, K. J. Coppersmith, *J. Geophys. Res.* **89**, 568 (1984).
7. J. Liu, Y. Klinger, K. Sieh, C. Rubin, *Geology* **32**, 649 (2004).
8. O. Zielke, J R. Arrowsmith, L. Grant Ludwig, S. O. Akçiz, *Science* **327**, 1119 (2010); published online 21 January 2010 (10.1126/science.1182781).
9. G. R. Noriega, thesis, University of California, Irvine (2009).
10. L. B. Grant, K. E. Sieh, *Bull. Seismol. Soc. Am.* **83**, 619 (1993).
11. L. B. Grant, K. E. Sieh, *J. Geophys. Res.* **99**, 6819 (1994).
12. J. Liu-Zeng, Y. Klinger, K. Sieh, C. Rubin, G. Seitz, *J. Geophys. Res.* **111**, B02306 (2006).
13. A. Schimmelmann, M. Zhao, C. C. Harvey, C. B. Lange, *Quat. Res.* **49**, 51 (1998).
14. A. Schimmelmann, C. B. Lange, B. J. Meggers, *Holocene* **13**, 763 (2003).
15. S. O. Akçiz, L. Grant Ludwig, J. R. Arrowsmith, *J. Geophys. Res.* **114**, B01313 (2009).
16. W. N. Engstrom, *Quat. Res.* **46**, 141 (1996).
17. See supporting material on *Science* Online.
18. D. R. Cayan, K. T. Redmond, L. G. Riddle, *J. Clim.* **12**, 2881 (1999).
19. G. R. Noriega, J. R. Arrowsmith, L. B. Grant, J. J. Young, *Bull. Seismol. Soc. Am.* **96**, 33 (2006).
20. L. B. Grant, *Science* **272**, 826 (1996).
21. S. O. Akçiz et al., *Eos* **87** (fall meet. suppl.), T21E-01 (2006).
22. Supported by NSF grants EAR 0409500 and 0711518, USGS grant 07HQGR0092, and the Southern California Earthquake Center (SCEC). SCEC is funded by NSF Cooperative Agreement EAR-0529922 and USGS Cooperative Agreement 07HQAG0008. The SCEC contribution number for this paper is 1305. Thanks to anonymous reviewers, student field assistants, L. Bidart for access to field sites, and J. Southon, M. Kirby, D. Cayan, K. Whipple, A. Heimsath, and E. Vivoni for discussions.

Slip in the 1857 and Earlier Large Earthquakes Along the Carrizo Plain, San Andreas Fault

Olaf Zielke,[1]* J Ramón Arrowsmith,[1] Lisa Grant Ludwig,[2] Sinan O. Akçiz[2]

The moment magnitude (M_w) 7.9 Fort Tejon earthquake of 1857, with a ~350-kilometer-long surface rupture, was the most recent major earthquake along the south-central San Andreas Fault, California. Based on previous measurements of its surface slip distribution, rupture along the ~60-kilometer-long Carrizo segment was thought to control the recurrence of 1857-like earthquakes. New high-resolution topographic data show that the average slip along the Carrizo segment during the 1857 event was 5.3 ± 1.4 meters, eliminating the core assumption for a linkage between Carrizo segment rupture and recurrence of major earthquakes along the south-central San Andreas Fault. Earthquake slip along the Carrizo segment may recur in earthquake clusters with cumulative slip of ~5 meters.

Recent earthquake ruptures along the North Anatolian fault in Turkey [moment magnitude (M_w) 7.4 Izmit earthquake, 1999] (1), the Kunlun Fault in China (M_w 7.8 Kokoxili earthquake, 2001) (2), the Denali fault in Alaska (M_w 7.9 Denali earthquake, 2002) (3), and the Longmenshan fault in China (M_w 7.9 Wenchuan earthquake, 2008) (4) present dramatic manifestations of large-earthquake phenomena, exemplifying the destructive potential of tectonically active faults. A primary step toward assessing the time and magnitude of future large earthquakes is the identification of earthquake recurrence intervals and along-fault slip-release patterns.

Previous work along the San Andreas Fault (SAF) (5, 6) reported that the largest slip associated with the surface rupture of the M_w 7.9 Fort Tejon earthquake of 1857—the most recent earthquake along the south-central SAF—occurred with ~9 m along the Carrizo segment (Fig. 1). Further investigation along the 1857 rupture trace (7) suggested that individual fault segments experienced essentially the same amount of slip in preceding earthquakes as they did in 1857 (e.g., the largest slip associated with preceding earthquakes occurred with ~9 m along the Carrizo segment). These and similar observations for the Wasatch fault in Utah led to the formulation of the uniform-slip and the characteristic earthquake model (7, 8), which dominate current